

## ANALYSIS OF BENDING CAPACITY OF COMPOSITE STEEL-CONCRETE SLABS WITH STEEL FIBER REINFORCED CONCRETE

Mindaugas Petkevičius<sup>1</sup>, Juozas Valivonis<sup>2</sup>

Vilnius Gediminas Technical University, Saulėtekio ave. 11, LT-10223 Vilnius, Lithuania  
E-mail: <sup>1</sup>[Mindaugas.Petkevicius@vgtu.lt](mailto:Mindaugas.Petkevicius@vgtu.lt); <sup>2</sup>[Juozas.Valivonis@vgtu.lt](mailto:Juozas.Valivonis@vgtu.lt)

**Abstract.** Analysis of experimental and theoretical results of investigations in strength of composite steel-concrete slabs is presented in this article. Profiled steel sheeting (*Holorib* type) and steel fibre reinforced concrete were used for specimens. For two slabs the layer of concrete was reinforced with steel fibre whereas the rest of them were not. Slabs were tested under static short-time load. The strength of composite slabs directly depends on the stiffness and the strength of the shear bond between the profiled steel sheeting and the concrete layer. Method for the strength analysis of horizontal section in composite slabs is based on the built-up bars theory. Influence of cracked concrete layer on strength of the structure and plastic deformation in compression zone of this layer are evaluated by this method. Furthermore, it evaluates the stiffness of separate layers and the stiffness of the shear bond between the profiled steel sheeting and the concrete layer. Experimental investigations were performed for determination of the shear characteristic for the bond between the steel sheeting and the concrete layer. Therefore specimens were made of the same concrete mixture as that of the slabs. Theoretical analysis of horizontal section for the composite slabs was made. Quite good agreement between theoretical and experimental results is obtained.

**Keywords:** strength, horizontal section, shear, contact, joint, composite slab, steel fiber, steel sheeting, concrete.

### Introduction

The most popular floor structure for the buildings in steel framework is composite steel-concrete slab. The strength and the stiffness of the joint between the profiled steel sheeting and the concrete layer influence the strength and the behaviour of such slabs. The strength of the joint between the layers depends on many factors, i. e. type and shape of profiled steel sheeting, quantity of embossments in the sheeting, thicknesses of sheeting and of concrete layer, distribution of loads, type of end anchorage and others.

The joint action of the layers in the composite steel-concrete slabs subjected to load can be achieved when the slip in the interface between the steel sheeting and the concrete is prevented. Adhesion and friction between the concrete and the metal not always ensures that the slip does not take place. The experimental investigations indicated that the failure of such slabs occurs in the contact zone at the supports with the slip between the concrete and the steel sheeting (de Andrade *et al.* 2004; Tenhovuori *et al.* 1996; Petkevičius 2009). The strength and the stiffness of this type of structure depend on the strength and the stiffness of the joint between the layers. Therefore ribs and indentations of various shapes are included in the thin-wall steel sheeting to get better con-

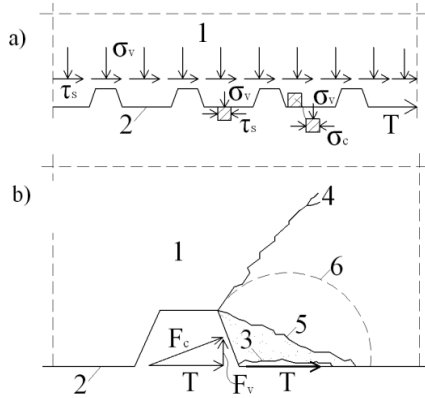
junction (bond) between the layers (Fig 1) (Mistakidis and Dimitriadis 2008). Use of these structural solutions helps to reduce the cost of the structure, to save concrete up to 30 %, good strength and stiffness of the structure is obtained, no need for formwork, quick erection, low height (depth) and weight of the structure (Dowling *et al.* 1997).



Fig 1. The embossments of the profiled steel sheeting

Performed theoretical and experimental investigations showed that it is very difficult to secure an absolutely stiff joint between the steel sheeting and the concrete. During operation especially when high stress acts

in the structure, the slip of the layers in relation to each is initiated. Using in specimens steel sheeting with various types of form irregularities (embossments) the failure mechanism of such slabs was determined by experimental investigations (Valivonis 2006).



**Fig 2.** Stress and strain state in the contact zone between the profiled steel sheeting and the concrete along the rib (Valivonis 2006): a – stress distribution along the ribs; b – stresses and mechanism of failure at the key on the rib: 1 – layer of concrete; 2 – rib in the sheeting; 3 – spall of concrete (wedge); 4 – crack due to the principal stress; 5 – destruction of concrete inner structure, cracks; 6 – plasticity zone

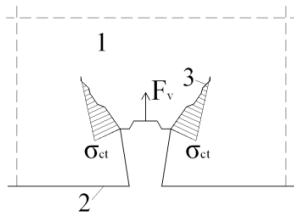


**Fig 3.** Distribution of load effects in transverse direction to of the rib (Valivonis 2006): 1 – layer of concrete; 2 – steel profiled sheeting; 3 – direction of the main crack

Due to bending of the composite slab in the contact zone along the steel sheeting rib the shear force  $T$  appears (Fig 2) which inflicts the local compressive stress  $\sigma_c$  at the key. When the compressive stress exceeds the concrete compressive strength the structure of the concrete disintegrates, cracks form wedge-shaped concrete surface via which the vertical and the horizontal forces are generated. Combined stress state appears therefore the structure fails when the principal tensile stress exceeds the tensile strength of the concrete (Fig 3). Such type of structure fails in the section between the support and the load applied.

### Theoretical carrying capacity analysis of flexural composite steel-concrete slabs

The method proposed for analysis of carrying capacity of the flexural composite steel-concrete slabs is based on built-up bars theory (Vainiūnas *et al.* 2006). It evalu-

ates the rigidity of separate layers, that of the joint between the concrete layer and the steel sheeting, also gives an opportunity to estimate the influence of the cracked concrete layer and of the compression zone plastic deformations in the concrete layer on the strength of the structure.

Experimental investigations show (Vainiūnas *et al.* 2006; Petkevičius 2009) that composite steel-concrete slabs fail in the horizontal section which is subjected to the action of the bending moment and the shear force along the span. Diagram for the analysis is shown in the Fig 4.

The carrying capacity of a flexural composite steel-concrete slab is determined by (Vainiūnas *et al.* 2006):

$$M_{Rd} = M_{pa} + T(x) \cdot z_{eff}. \quad (1)$$

Here  $M_{pa}$  – the plastic bending moment carried by the profiled steel sheeting.

Lever arm of the internal forces is determined by:

$$z_{eff} = d_p - \frac{x_m}{2}. \quad (2)$$

Value of the shear force  $T(x)$  for any interval of the horizontal section may be estimated by the following equation:

$$T(x) = \frac{M_R(x) \cdot z_{eff}}{\gamma (E_p I_p + E_{c,eff} I_{c,eff})} \cdot k(x). \quad (3)$$

Here  $M_R(x)$  – carrying capacity of composite member assuming that the joint between the layers is absolutely stiff;  $E_p, I_p$  – elasticity modulus and the second moment of area for the steel sheeting;  $E_{c,eff} = \omega \cdot E_{cm}$  – concrete elasticity modulus with allowance for its plastic deformations (sometimes referred to as modulus of deformation).

By experimental investigations (Zalesov *et al.* 2002) it was determined that the tension zone of the concrete layer of structures reinforced with the external reinforcement is restrained and therefore the width and the spacing of the normal cracks are reduced. Thus the second moment of area  $I_{c,eff}$  for a composite slab with allowance for the cracked concrete layer is determined by formula:

$$I_{c,eff} = \frac{b_w \cdot x_m^3}{3} + \frac{(b - b_w) \cdot h_c^3}{12} \cdot \left[ 1 + 12 \left( \frac{x_m}{h_c} - 0.5 \right)^2 \right]. \quad (4)$$

The average compression zone depth is obtained from such expression:

$$x_m = d_p \left( \sqrt{\mu^2 + \frac{\mu \cdot h}{d_p}} - \mu \right), \quad (5)$$

here

$$\mu = \mu_f + \frac{E_p \cdot A_p}{E_{c,eff} \cdot b_w \cdot d_p}, \quad (6)$$

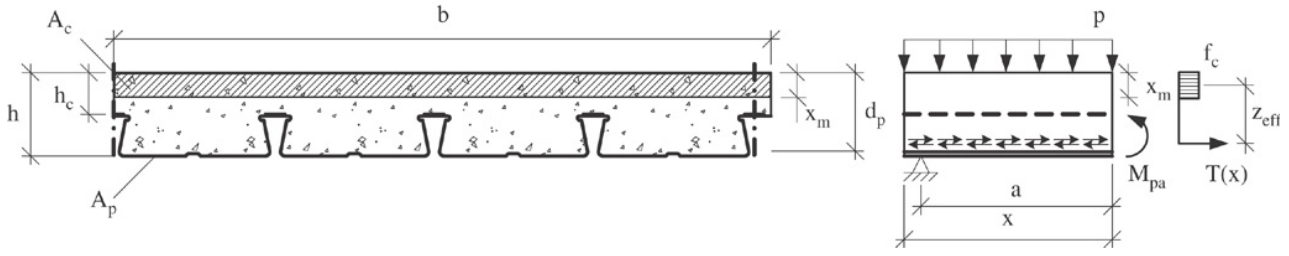


**Fig 4.** The distribution of stresses in horizontal section of composite slab (Vainiūnas *et al.* 2006)

$$\mu \cdot h = \mu_f \cdot h_c + \frac{2 \cdot E_p \cdot A_p}{E_{c,eff} \cdot b_w}, \quad (7)$$

$$\mu_f = \frac{b \cdot h_c}{b_w \cdot d_p}. \quad (8)$$

The rigidity of the layers is definable as follows:

$$\gamma = \frac{1}{E_p A_p} + \frac{1}{E_{c,eff} A_{c,eff}} + \frac{z_{eff}^2}{E_p I_p + E_{c,eff} I_{c,eff}}. \quad (9)$$

Yielding of the layers and the slab loading case are taken into account by the coefficient  $k(x)$ .

For the uniformly distributed load:

$$k(x) = 1 - \frac{2(ch(0.5\lambda \cdot l) - ch(\lambda(0.5l - x)))}{x \cdot \lambda^2(l - x) \cdot ch(0.5\lambda \cdot l)}. \quad (10)$$

For the case of two concentrated loads and  $x \leq a$ :

$$k(x) = 1 - \left[ \frac{ch(\lambda(0.5l - a))}{(x \cdot \lambda) \cdot ch(0.5\lambda \cdot l)} \cdot sh(\lambda \cdot x) \right]. \quad (11)$$

For the case of two concentrated loads and  $x < a$ :

$$k(x) = 1 - \left[ \frac{ch\lambda(0.5l - x)}{(a \cdot \lambda) \cdot ch(0.5\lambda \cdot l)} \cdot sh(\lambda \cdot a) \right]. \quad (12)$$

Here  $l$  – design length of the structure;  $a$  – distance between support and the load application point;  $x$  – distance between the end of the slab and the section the strength of which is to be determined;  $sh$  and  $ch$  – hyperbolic sine and hyperbolic cosine.

Coefficient  $\lambda$  defines the rigidity of the joint between the layers which depends on the rigidity of the individual layers and the shear rigidity of the joint between the layers:

$$\lambda = \sqrt{\alpha \cdot \gamma}. \quad (13)$$

Coefficient  $\alpha$  evaluates the rigidity of the contact between the steel sheeting and the concrete layer.

For the composite slab with the usual concrete layer:

$$\alpha = \frac{b \cdot G_w}{z_{eff}}. \quad (14)$$

Concrete strength is increased by its reinforcing with the steel fibre. Investigations conducted by the other authors (Рабинович 2004; Šalna and Marčiukaitis 2007) and by us revealed that the shear strength of concrete increases up to 1.5 times by steel fibre reinforcement. Also one knows that the concrete shear strength is 1.5–2.0 times greater than its tensile strength. Taking in to consideration these assumptions for the composite slab reinforced with the steel fibre the rigidity of the joint between the layers can be determined in such a way:

$$\alpha = 1.5 \cdot \frac{f_{sfrct}}{f_{ct}} \cdot \frac{b \cdot G_w}{z_{eff}}. \quad (15)$$

Here  $f_{ct}$ ,  $f_{sfrct}$  – the tensile strength of the usual concrete and the concrete reinforced with the steel fibre, respectively.

Shear rigidity characteristic  $G_w$  for the contact zone between the layers is determined from the experimental investigations performed by the author of this paper.

### Experimental investigation of the joint between the profiled sheeting and the concrete layer

Experimental investigations were performed to gain information for effective evaluation of strength and behaviour for the joint between the steel sheeting and the concrete layer. The specimens (Fig 5) were made of analogous steel sheeting and of the same mixture of the normal weight concrete as the slabs P1, PF2, P3, PF4. Two parties of eight specimens were made at the first and the second concreting. During one concreting concrete of four specimens were reinforced with the steel fibre, concrete for the rest specimens were not reinforced.

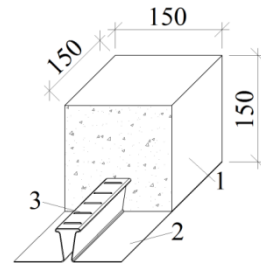


**Fig 5.** General view of the specimen for determination of the rigidity for the joint between the layers: 1 – concrete; 2 – profiled steel sheeting; 3 – transverse rib (embossment)

Test arrangement diagram for determination of the strength and the rigidity for the joint between the layers are shown in the Fig 6. Specimens were tested under the static short-time load. Load was raised by stable rate with the use of a hydraulic jack. The displacements of steel sheeting and concrete were measured during the test.

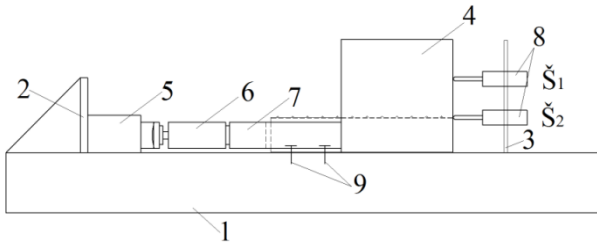


**Fig 6.** Test arrangement diagram for strength and stiffness determination of the joint between the layers: 1 – bed; 2 – abutment for hydraulic jack; 3 – support for fixing shear devices; 4 – specimen; 5 – hydraulic jack; 6 – electronic dynamometer; 7 – steel U profile for transferring the force to the concrete; 8 – displacement measuring devices; 9 – bolts for fixing the specimen to the bed

Relationships between the shear force and the shear strain were established by tests. Comparison of the average relationships for all specimens is illustrated in the Fig 8.

Analysis of proposed relationships (Fig 8) shows that the specimens with the usual concrete layer behave elastically until the ultimate shear force is reached. At this stage the chemical adhesion and transverse ribs (embossments) provide usual performance for the concrete layer and the steel sheeting joint. The chemical adhesion may be disrupted when the horizontal slip due to action of the tangential shear force takes place. Combined state of stress appears at the (transversal) embossments and when tension stress exceeds concrete tension strength the cracks form, then the concrete layer is separated from the steel sheathing and failure takes place (Fig 7). The failure is sudden and fragile.

Failure of the specimens with the layer of concrete reinforced by the steel fibre is plastic (Fig 8). Results of tests showed that the chemical adhesion fails till  $\sim 0.05F_u$  (here  $F_u$  is the failure shear force for the specimens) and the local compressive stress occurs at the transversal embossments. The rate of the horizontal displacement increase with the load is reduced due to the restraint of transversal deformations of the concrete layer offered by the steel fibre. When the load value of  $\sim 0.8-0.9F_u$  is reached the rate of the horizontal displacement starts to grow substantially. At this stage the local compression stress at the transversal embossments approaches the concrete compression strength. When the compression stress at the embossments exceeds the concrete compression strength, the wedge is formed then the shear force action tends to separate the concrete layer from the steel sheeting and when the tension strength of the concrete reinforced with the steel fibre is exceeded the cracks open

and failure in the horizontal section takes place. The specimens failed plastically.

The investigations revealed that joint between the profiled steel sheeting and the layer of the concrete reinforced with steel fibre is  $\sim 46-50\%$  stronger than that of the specimens with the usual concrete layer.

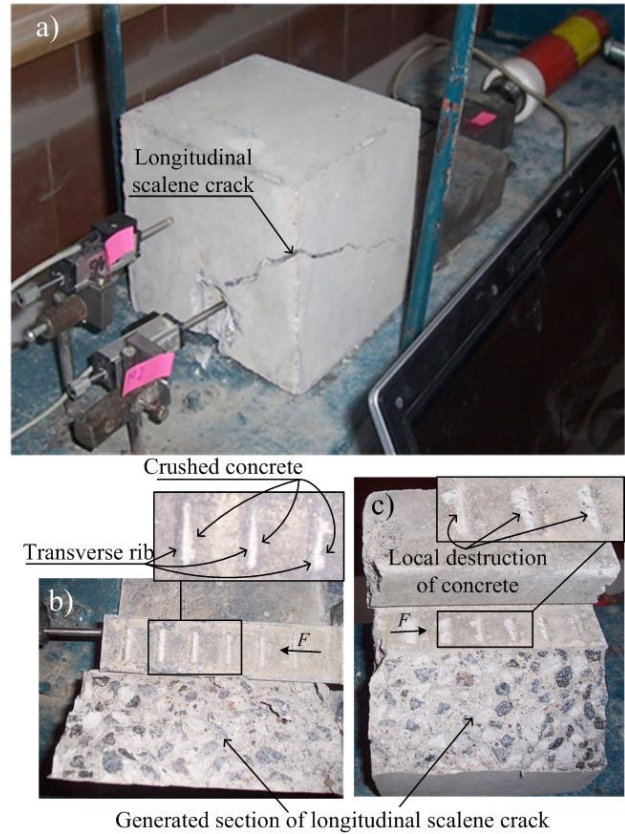


**Fig 7.** Specimen for determination of the strength and the rigidity of the joint between the layers: a – general view of the specimen after its failure in the test arrangement; b – transversal embossments on the steel sheeting after failure; c – crushed concrete near the transversal embossments on the steel sheeting after failure

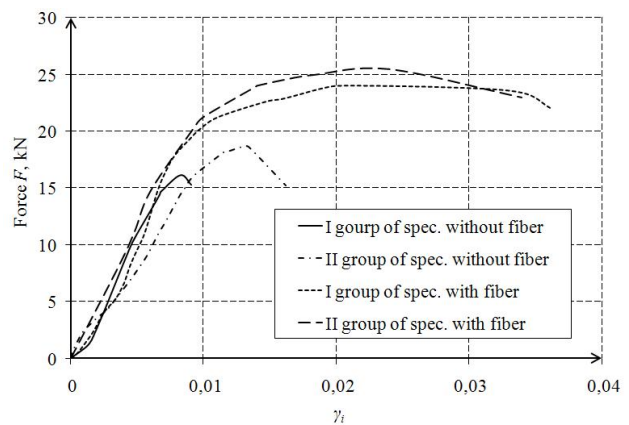


**Fig 8.** Average shear force to shear strain relationships for all tested specimens

## Experimental investigation of composite steel-concrete slabs

Four composite steel-concrete slabs were prepared for investigations. “Swallow tail” CS48-36-750 ZN0.9 type steel sheeting of the firm STEELCOMP was used for manufacture of the specimens. Crushed granite (5–11 mm), quartz sand (0–5 mm) and Portland cement were used for the concrete mixture. Steel fibre TF HE 50/1.0 of type, quantity of fibre was 20 kg/m<sup>3</sup> of concrete.

Two batches for concreting were produced. From each batch two slabs were manufactured. In one batch concrete layer for one slab was reinforced with the steel fibre and for the other one it was not. The depths of all the slabs are presented in the Table 1.

From each batch control specimens were made for determination of mechanical properties of materials. The average values of the mechanical characteristics obtained are given in the Table 1. The test arrangement diagram is presented in the Fig 9. The slabs were tested with the static short-time load. Two concentrated loads were applied at 1/3 of the span. The load was increased by stable rate by the means of a hydraulic jack. Transversal, longitudinal, shear deformations and deflections were measured during the test. Longitudinal tension (at the bottom of the slab) and compression (at the top of the slab) deformations were measured at the middle of the span. Transversal deformations of the concrete were measured at the top of the slab on the rib of the steel sheeting at the supports. Shear deformations were measured at the ends of the slab. Deflection of the slab was measured at the middle of the span.

Two groups of specimens made in the first and the second concreting were tested according to the diagram shown in the Fig 9. Results for each group are presented in the separate graphs. Using results recorded by test devices shear deformations to bending moment and transversal deformations to bending moment relationships were drawn.

Analysis of the experimental investigations results (Fig 12) points out that the composite slabs P1 and P3, the concrete layer of which is without steel fibre, behave elastically up to 0.368–0.385 $M_R$ . Composite slabs PF2 and PF4, the concrete layer of which is reinforced with steel fibre, behave elastically up to 0.442–0.486 $M_R$  (here  $M_R$  is the failure moment of the slabs). The slip in the composite slabs with the concrete layer reinforced by the steel fibre begins at the load ~ 50–60 % higher than that for the composite slabs with the usual concrete layer. When the bending moment exceeds 0.368–0.385 $M_R$  for the slabs P1, P3 and 0.442–0.486 $M_R$  for the slabs PF2, PF4 the chemical adhesion in the contact between the steel sheeting and the concrete layer fails, displacement of the layers in relation to each other begins (Fig 12). The local compressive stress occurs at the embossments of the steel sheeting. The failure of the composite steel-concrete slab in the horizontal section is possible when the chemical adhesion fails with either cutting off the transversal ribs (embossments) or overleaping of the concrete layer over the transversal embossments of the steel sheeting. Since the lifting of the concrete layer is restrained by the

shape of the longitudinal ribs and the transversal embossments of the profiled steel sheeting then in the concrete layer at the transversal embossments combined state of stress appears. Above the steel sheeting vertical and horizontal deformations in the transversal direction occur. When the bending moment in the slabs P1, P3 exceeds  $M \sim 0.4M_R$  and in the slabs PF2, PF4 exceeds  $M \sim 0.5M_R$  the shear deformations develop substantially (Fig 12) also transversal deformations above the longitudinal ribs of the steel sheeting increase significantly (Fig 13). The principle tension stress in the concrete layer makes angle of ~45° with the vertical to the slab. When the tension stress exceeds the tension strength of the concrete the longitudinal cracks open (Fig 10).

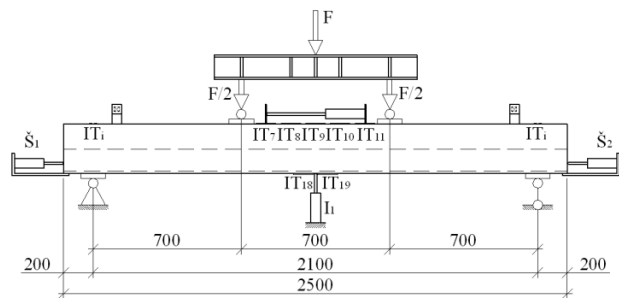


Fig 9. Test arrangement scheme

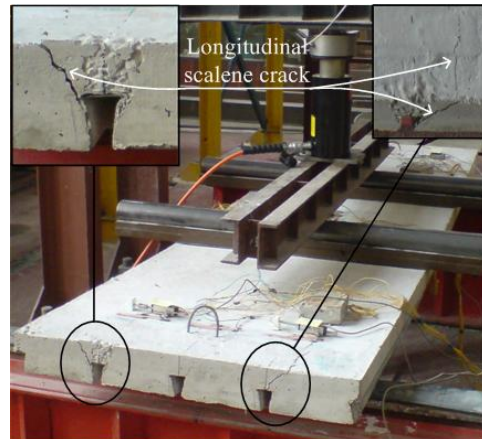


Fig 10. Composite steel – concrete slab in the test setup after the failure



Fig 11. Slip between the layers in a composite steel – concrete slab

**Table 1.** Characteristics of the composite slabs

Specimen no.	Width of the slab, $b$ (m)	Distance from the end of the slab to the critical section, $x$ (m)	Distance from the support to the load application point, $a$ (m)	Design length, $l$ (m)	The shear characteristic in the elastic stage, $G_v$ (Mpa)	Cross-section depth of the slab, $h$ (m)	Concrete layer depth above the steel sheeting rib, $h_c$ (m)	Profiled steel sheeting cross-sectional area, $A_p$ (m <sup>2</sup> )	Concrete elasticity modulus, $E_{cm}$ (GPa)	Steel elasticity modulus, $E_s$ (GPa)	Concrete cylindrical strength, $f_c$ (Mpa)	Steel yield strength, $f_y$ (MPa)
P1	0.75	0.90	0.70	2.10	88	0.1017	0.0552	$1.01 \times 10^{-3}$	27.71	210	31.28	413.0
PF2	0.75	0.90	0.70	2.10	88	0.1023	0.0558	$1.01 \times 10^{-3}$	30.29	210	32.09	413.0
P3	0.75	0.90	0.70	2.10	83	0.1012	0.0547	$1.01 \times 10^{-3}$	33.46	210	33.79	413.0
PF4	0.75	0.90	0.70	2.10	83	0.1075	0.0610	$1.01 \times 10^{-3}$	31.23	210	34.32	413.0

**Table 2.** Comparison of theoretical and experimental results of the strength for the horizontal section

Specimen no.	Plastic bending moment of the profiled steel sheeting, $M_{pa}$ (kNm)	Shear force, $T(x)$ (kN)	Carrying capacity of flexural slabs obtained by experiments, $M_{Rd}$ (kNm)	Carrying capacity of flexural slabs obtained from theory, $M_R$ (kNm)	Ratio of theoretical to experimental values
					$M_{R,call} / M_{R,obs}$
P1	3.40	358.0	25.91	27.55	1.06
PF2	3.40	367.9	32.20	28.58	0.89
P3	3.40	357.5	28.28	27.75	0.98
PF4	3.40	369.9	33.99	30.35	0.89

Direction of the longitudinal cracks adjusts to that of the principle stress. When the load reached  $0.9-0.95M_R$  in the concrete layer above the longitudinal ribs of the steel sheeting the longitudinal cracks were observed. They extended from the end of the slab up to the load application place. The width of the longitudinal cracks in the slabs PF2, PF4 (concrete reinforced with the steel fibre) was much less than that in the slabs P1, P3 since the steel fibre restrained the transverse deformations produced by the tension stress.

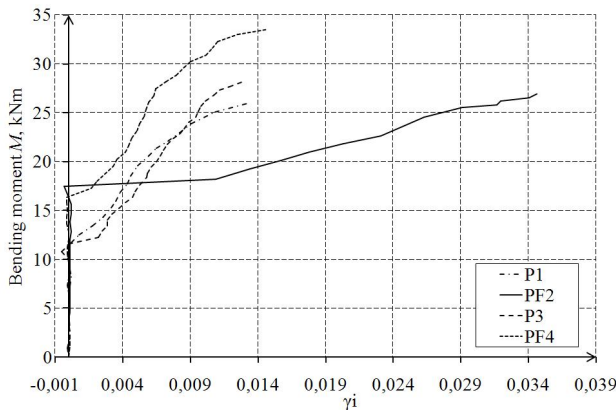


**Fig 12.** The shear deformations in the contact zone related to the bending moments for the slabs P1, PF2, P3, PF4

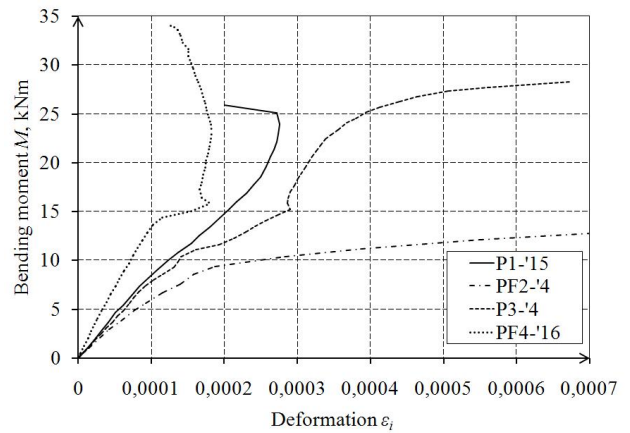


**Fig 13.** Transverse deformations over the longitudinal ribs of the sheeting related to the bending moments for the slabs P1, PF2, P3, PF4

Performance of all slabs up to  $(0.368-0.385M_R)$  the load, at which the layers of the slabs P1, P3 begin to displace in relation to each other, almost does not differ (Fig 12). When the bending moment in the slabs PF2, PF4 exceeds  $M \sim 0.4M_R$  the steel fibre in the concrete acts together with the concrete. It results in the concrete tension strength increase. Therefore the longitudinal inclined cracks in the concrete layer above the longitudinal ribs do not open. The compression strength of the

concrete in the combined state of stress at the transversal embossments is used more effectively; the joint between the layers becomes stronger and stiffer. The said above affects the elastic performance under the action of a greater load.

Character of the failure of all composite slabs P1, PF2, P3, PF4 was the same. The failure took place in the horizontal section. At the failure the longitudinal cracks formed (Fig 10), they extended from the end of the slab up to the cross-section at which the concentrated load was applied (at the distance of 900 mm). The slabs PF2, PF4 failed in more plastic way than the slabs P1, P3 did. The width of the longitudinal cracks inclined at the angle of  $\sim 45^\circ$  was less in the slabs PF2, PF4 than that in the slabs P1, P3. Horizontal displacement of 0.5–4 mm for the sheeting was recorded (Fig 11). Different values of the failure loads of different specimen groups were obtained (Table 2).

### Analysis of theoretical and experimental results of carrying capacity for flexural composite steel-concrete slabs

Theoretical determination of carrying capacity executed using the method proposed in (Vainiūnas *et al.* 2006).

Characteristic  $G_w$  for the concrete to steel sheeting joint used in analysis performed was established by the specimens tested for rigidity of the joint between the layers (Fig 8).

Carrying capacity was determined by the formula (1) using the actual mechanical characteristics of materials and the actual dimensions of the slabs presented in the Table 1. The second moment of area of the cracked concrete layer was calculated by formulas (4–8). The coefficient  $\alpha$  which evaluates the rigidity of the joint between the layers for the composite slabs with the usual concrete layer was determined by the expression (14) and for the slabs with the concrete layer reinforced by the steel fibre according to the formula (15). The shear force resisted by the joint between the steel sheeting and the concrete layer for estimation of strength is determined by the formula (3).

Analysis of theoretical experimental results shows that the values of carrying capacity obtained by the proposed (Vainiūnas *et al.* 2006) method are close to the experimental ones. Obtained results are given in the Table 2. The proposed method evaluates the effect of the shear force on the performance of the joint between the steel sheeting and the concrete layer.

### Conclusions

For the theoretical analysis of the carrying capacity of the composite steel-concrete slabs the method based on build-up bars theory (Vainiūnas *et al.* 2006) was used. The method takes into account the influence of the shear force on the carrying capacity of the composite steel-concrete slabs. Advantage of this method is that the shear force  $T(x)$  acting in the contact between the layers can be determined in analytical way. In calculation of the shear

force  $T(x)$  the partial stiffness of the joint between the steel sheeting and concrete layer is evaluated.

The experimental investigations of the composite steel-concrete slabs were performed. The slip in the slabs with the concrete layer reinforced by the steel fibre begins at  $\sim 50$ – $60$  % higher acting load than in the slabs with the usual concrete layer (Fig 11). All slabs failed in the horizontal section between the layers. The longitudinal cracks formed (Fig 10). The width of the longitudinal cracks in the slabs with the concrete layer reinforced by the steel fibre was substantially less than that in the slabs with the usual concrete layer. Recorded displacement of the steel sheeting in relation to the concrete layer equals to 4 mm (Fig 11). The joint between the layers of all tested slabs was of the partial stiffness. The specimens of the joint with the concrete layer reinforced by the steel fibre failed plastically and they are  $\sim 46$ – $50$  % stronger than the specimens without the fibre, the failure of which was sudden and brittle (Fig 8).

Results of investigation of the joint (Fig 8) and relationships of the shear deformation to the bending moment for the slabs (Fig 12) demonstrate that the steel fibre affects the increase in the carrying capacity of the flexural composite slabs. The tension strength of the concrete enhanced by the steel fibre affects the increase in the shear strength of the concrete. For evaluation of the stiffness for the joint between the steel sheeting and the concrete layer reinforced by the steel fibre the expression (15) is proposed on the basis of experimental investigations

Agreement of the results of analysis to the experimental ones is sufficiently good. Ratio of the theoretical values to the experimental ones varies within the limits of  $M_{R,call} / M_{R,obs} = 0.98$ – $1.06$  for the slabs with the usual concrete layer and the ratio of  $M_{R,call} / M_{R,obs} = 0.89$  for the slabs with the concrete layer reinforced by the steel fibre.

### References

- de Andrade SAL; da S Vellasco PCG; da Silva JGS; Takey TH. 2004. Standardized composite slab systems for building constructions, *Journal of Constructional Steel Research* 60: 493–524. doi:10.1016/S0143-974X(03)00126-3
- Bode, H.; Minas, F.; Sauerborn, I. 1996. Partial connection design of composite slabs, *Journal of Structural Engineering International* 6(1): 6–53.
- Burnet, M. J.; Oehlers, D. J. 2004. Rib shear connectors in composite profiled slabs, *Journal of Constructional Steel Research* 57: 67–87.
- Dowling, P. J.; Burgan, B. A. 1997. Steel structures in the new millennium, *Statyba – Civil Engineering* 4(12): 5–19.
- Mistakidis, S.; Dimitriadis, G. 2008. Bending resistance of composite slabs made with thin-walled steel sheeting with indentation or embossments, *Thin-walled structures* 46: 192–206. doi:10.1016/j.tws.2007.08.001
- Motak, J.; Machacek, J. 2004. Experimental behaviour of composite girders with steel undulating web and thin-walled shear connector's hilti stripcon, *Journal of Civil Engineering and Management* 10(1): 9–45.
- Petkevičius, M. 2009. Kompozitinių plienbetoninių plokščių armuotų plieniniu plaušu savybių tyrimas [Analysis of

- behavior of composite steel and steel fiber reinforced concrete slabs], *Mokslas – Lietuvos ateitis* 1(5): 50–55.
- Šalna, R.; Marčiukaitis, G. 2007. The influence of shear span ratio on load capacity of fibre reinforced concrete elements with various steel fiber volumes, *Journal of Civil Engineering and Management* 13(3): 209–215.
- Tenhovuori, A.; Karkkainen, K.; Kanerva, P. 1996. Parameters and definitions for classifying the behaviour of composite slabs, in *Proc. of an engineering foundation conference—composite construction in steel and concrete*.
- Vainiūnas, P.; Valivonis, J.; Marčiukaitis, G.; Jonaitis, B. 2006. Analysis of longitudinal shear behaviour for composite steel and concrete slabs, *Journal of Constructional Steel Research* 62: 1264–1269. doi:10.1016/j.jcsr.2006.04.019
- Valivonis, J. 2006. Analysis of behaviour of contact between the profiled steel sheeting and the concrete, *Journal of Civil Engineering and Management* 12(3): 187–194.
- Vaškevičius, A.; Marčiukaitis, G.; Valivonis, J. 2001. Lenkiamųjų kompozitinių elementų, armuotų profiliuotais metalo lakštais, darbo analizė [Analysis of behavior of composite elements with corrugated steel sheet], *Statyba – Civil Engineering* 7(6): 1392–1525.
- Zalesov, A. S.; Muchanediiev, T. A.; Cistekov, E. A. 2002. Calculation of deflections reinforced concrete structures according new standards, *Concrete and Reinforced Concrete* 6: 12–20.
- Рабинович, Ф. Н. 2004. *Композиты на основе дисперсно армированных бетонов: Вопросы теории и проектирования, технология, конструкции: Монография* [Composite materials based on fiber reinforced concretes. Theory, design and technology, structures: Monography]. Moscow: ACV. 560 p.
- Ржаницин, А. 1986. *Составные стержни и пластинки* [Build-up bars and panels]. Moscow: Stroizdat. 316 p.